Two and three-dimensional pressure-impulse models of wave impact on structures.

Deborah J. Wood † and D. Howell Peregrine ‡

Abstract

For violent wave impacts against sea walls and breakwaters Cooker and Peregrine (1990,1992) suggest the use of a pressure-impulse model. Here the model is used for three-dimensional examples.

1. Introduction

When a wave is breaking or near breaking when it hits a wall then very high, short lived, pressures can occur. Though this peak in pressure occurs for only a short period of time the magnitude is often many times larger than any other pressures associated with the impact, and maybe enough to cause damage to a structure such as a sea wall or breakwater. This peak in pressure is quite difficult to predict because, as Bagnold noted (Bagnold, 1939), pressures for similar waves vary considerably, whereas pressure impulse (the integral of pressure with respect to time, over the duration of the impact) has less variation.

Pressure impulse, as given in Lamb (1932) and Batchelor (1967), has been used to provide a theoretical model for wave impact by Cooker and Peregrine (1990, 1992, 1995). Chan (1994) and Losada, Martin and Medina (1995) have shown that this theory compares well with experiment. Pressure impulse theory has been further used for impacts in containers (Topliss, 1994) and impacts under a deck (Wood and Peregrine, 1996). A useful property of pressure-impulse theory is the relative insensitivity to the geometry of the problem.

†Research assistant, School of Mathematics, University of Bristol, University Walk, Bristol, BS8 1TW, UK, (*Deb.Wood@bristol.ac.uk*)

‡Professor of Applied Mathematics, School of Mathematics, University of Bristol, (*D.H.Peregrine@bristol.ac.uk*)

Many theoretical and experimental studies of wave impact on a vertical wall are two-dimensional. However, it is clear that for a wave impacting on a structure, such as a breakwater, the impact is rarely two-dimensional. Nevertheless, if the wave crest is sufficiently wide at impact then the impact can be considered to be two-dimensional towards the centre of the wave. This is where the highest pressures are expected to occur. Here we present three-dimensional examples which can be used directly, or to judge when the two-dimensional result is adequate.

2. Pressure impulse

Let p be the excess pressure over atmospheric. The pressure impulse P is defined by

$$P = \int_{t_1}^{t_2} p\,dt, \tag{1}$$

where t_1 and t_2 are the times just before and after impact respectively.

Choosing units made dimensionless with the water density, ρ, a typical impact velocity, U, and length scale, H, the total depth of water at impact, we follow Cooker and Peregrine (1990, 1992, 1995) and simplify the equation of motion to

$$\frac{\partial \mathbf{u}}{\partial t} = -\nabla p, \tag{2}$$

for the short time interval, Δt, of the impulse, when for almost all the velocity field the rate of change of velocity, $\mathbf{u}$, is the dominant term. Integration with respect to time over the duration of the impact gives:

$$\mathbf{u}_2 - \mathbf{u}_1 = -\nabla P, \tag{3}$$

where $\mathbf{u}_2$ and $\mathbf{u}_1$ are the velocities after and before impact respectively. Now we assume the water is incompressible before and after impact, and so we have $\nabla.\mathbf{u}_2 = \nabla.\mathbf{u}_1 = 0$. Therefore we need to solve

$$\nabla^2 P = 0 \tag{4}$$

in the fluid domain, subject to appropriate boundary conditions.

The boundary conditions can be grouped into three different types:

1)At the free surface the $p = 0$, so

$$P = 0. \tag{5}$$

2)At points on a rigid boundary where impact occurs the velocity component perpendicular to the boundary is taken to be zero after impact, and some function of position, V, before impact. Using the normal component of equation (3) we find:

$$\partial P/\partial n = V, \tag{6}$$

where n is in the normal direction to the surface pointing into the fluid. We often choose V to be uniform in space, for want of better information, as a reasonable simplifying assumption. Then, choosing V to be the velocity scale U, and to be in the direction towards the wall, equation (6) simplifies to give:

$$\partial P/\partial n = -1. \tag{7}$$

3)At points on a fixed rigid boundary where no impact occurs the velocity normal to the boundary is zero both before and after impact, and thus

$$\partial P/\partial n = 0. \tag{8}$$

The far-field condition is that $P \to 0$.

Hence, to find a pressure-impulse model for an impact problem we must solve Laplace's equation subject to these boundary conditions. In this paper P is non-dimensional, to get back to dimensional quantities simply multiply P by ρUH. Note that since accelerations are assumed much greater than gravity, see equation (2), this approach only applies to violent impacts.

3. Impact on a wall.

Chan (1994), figure 19, examines the model from Cooker and Peregrine (1990, 1992) and looks at plots of pressure impulse down the wall, varying the depth of water but keeping the impact region size constant. As the water depth becomes the large, there is a 'tail' to the pressure impulse distribution down the wall. Cooker and Peregrine (1995) gives the infinite depth solution, which when integrated gives logarithmic divergence giving a total impulse that is infinite. This shows that for deep water cases this model is inadequate. This emphasises the importance of examining three-dimensional effects.

3.1. Three-dimensional impact on a wall.

Consider the impact of a body of water on a patch of a wall. Cooker and Peregrine (1995) noted that unless the width of the impacting water is quite small the actual shape of the wave away from the impact region is relatively unimportant. So we simplify the free surface to be horizontal and let A denote the area of the patch. We use the boundary conditions described in section 2. On the free surface the usual condition of $P = 0$ is required. The patch is where impact takes place so we need $\partial P/\partial y = V(x, z)$, with y in the direction normal to the patch and into the water, with x and z as shown in figure 1. On the rest of the wall no impact occurs so we require $\partial P/\partial y = 0$. Along the bottom of the region of the fluid, on $z = -1$, we have a solid boundary so $\partial P/\partial z = 0$. We also need $P \to 0$ as we move far away from the impact patch. So a solution to Laplace's equation subject to the boundary conditions shown in figure 1 is required.

We can solve this problem in terms of a Fourier series expansion and a Fourier integral. The boundary conditions on the planes $z = 0$ and $z = -1$ enable the separation of the z dependence giving an expression for P:

$$P(x, y, z) = \sum_n P_n(x, y) \sin(\lambda_n z), \tag{9}$$

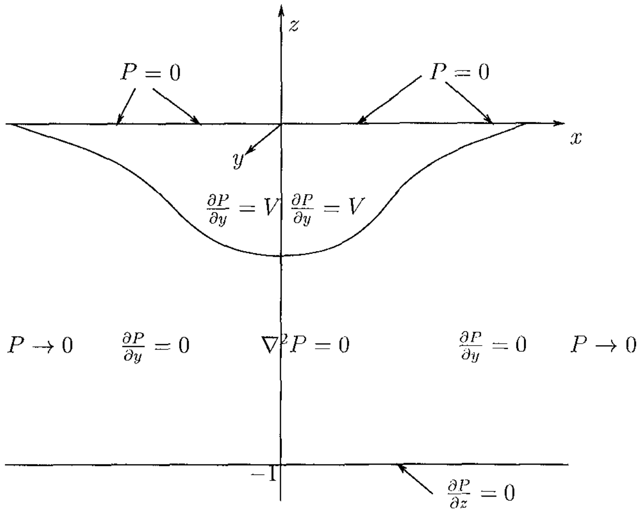

Figure 1: Impact on a patch of a wall. View facing wall.

where $\lambda_n = (n + 1/2)\pi$. A Fourier transform of the problem is taken in the x direction. We assume that the patch is symmetric about $x = 0$ for simplicity. Hence the Fourier cosine transform is defined as:

$$\overline{P_n}(k, y) = \int_{-\infty}^{\infty} P_n(x, y) \cos(kx) dx. \tag{10}$$

The boundary condition on the impact patch becomes:

$$\sum_n \frac{\partial P_n(x, 0)}{\partial y} \sin(\lambda_n z) = V(x, z). \tag{11}$$

Multiply by $\sin(\lambda_r z)$ and integrate with respect to z:

$$\frac{\partial P_r(x, 0)}{\partial y} = 2 \int V(x, z) \sin(\lambda_r z) dz, \tag{12}$$

where the integration in z is, for a given x, over values of z on the patch. Finally we transform this equation in x to give:

$$\frac{\partial \overline{P_n}(k, 0)}{\partial y} = 2 \int \int_A V(x, z) \sin(\lambda_n z) \cos(kx) dz dx, \tag{13}$$

where the integration is over the patch area A.

The transform in x of Laplace's equation leads to:

$$\frac{\partial^2 \overline{P_n}}{\partial y^2} - (k^2 + \lambda_n^2)\overline{P_n} = 0. \tag{14}$$

To simplify the notation we use $m^2 = (k^2 + \lambda_n^2)$. In future expressions it must be remembered that m is dependent on k and n. We require $P(x, y, z) \to 0$ as $y \to \infty$, which means that solving equation (14) gives:

$$\overline{P_n}(k, y) = A_n(k)\mathrm{e}^{-my}, \tag{15}$$

where $A_n(k)$ are functions of k, to be found using the boundary condition at the wall. Then equations (13) and (15) give:

$$A_n(k) = -\frac{2}{m}\int\int_A V(x, z)\sin(\lambda_n z)\cos(kx)dxdz. \tag{16}$$

The final step is to take the inverse transform of equation (15) and substitute into equation (9) to obtain the Fourier sum for P:

$$P(x, y, z) = \sum_n \frac{1}{\pi}\int_0^\infty A_n(k)\mathrm{e}^{-my}\sin(\lambda_n z)\cos(kx)dk, \tag{17}$$

with $A_n(k)$ given by equation (16).

Next consider the specific case of a rectangular patch of depth d and width $2a$ (symmetric about $x = 0$). $V(x, z) = -1$ on the patch. Now we can carry out the integration in equation (16) directly to obtain

$$A_n(k) = -\frac{4}{k\lambda_n m}\sin(ka)\left[1 - \cos(\lambda_n d)\right]. \tag{18}$$

Using (17), for this specific case, we obtain the Fourier sum for P:

$$P(x, y, z) = -\sum_n \frac{4}{\pi\lambda_n}\left[1 - \cos(\lambda_n d)\right] I(n, x, y)\sin(\lambda_n z), \tag{19}$$

where

$$I(n, x, y) = \int_0^\infty \frac{\sin(ka)\cos(kx)\mathrm{e}^{-(k^2+\lambda_n^2)^{1/2}y}dk}{k(k^2 + \lambda_n^2)^{1/2}}. \tag{20}$$

To evaluate pressure impulse for this problem the Fourier series must be truncated. For a patch of height 0.1 the difference between taking 20 and 50 terms is only 4% and for a patch of height 1, the difference is substantially less. The integration is carried out using NAG routine D01ASF, which treats the integral as a Fourier cosine transform. This enables us to evaluate pressure impulse for this problem. Of particular interest are the contours of pressure impulse on the wall itself, as shown in figure 2 for a patch of height 0.2 and width 2.

The total impulse is 1.085 and 0.085 for patches of width 2 and depths 1 and 0.2 respectively. If integration is only taken over the central width $2a$ then

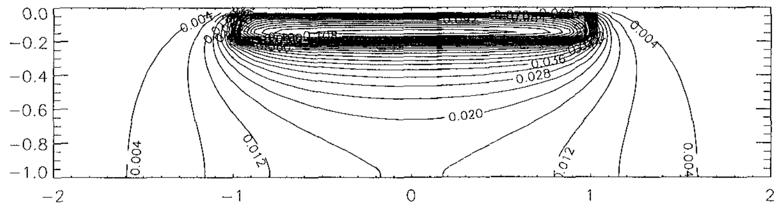

Figure 2: Pressure-impulse contours for impact on a patch of a wall where the patch covers the top 20% of the wall below the water level and is width 2.

the corresponding values are 0.878 and 0.074. As expected the larger the area of impact the larger the total impulse. Figure 3 shows a plot of total impulse against depth of water (the total impulse has been temporarily been scaled to have depth of impact 1 as our length scale H, to compare with Chan (1994)), where the integration is over the central width of $2a$, and the impact region is the top distance 1. We note that the total impulse seems to tend to a finite value instead of increasing with depth of water below the impact region, as predicted by the two-dimensional solution. It is more realistic that as the depth of water at the wall becomes very deep that the total impulse tends to a finite value.

Figure 4 shows a comparison of the pressure impulse on the wall for the two-dimensional impact model and down the centre line of the three-dimensional 'patch' model. For the comparison impact on the top 20% of the depth of water is used. Even when the patch width is twice the water depth at the wall the 'patch' model shows a lower pressure impulse down the centre line than is found using the two-dimensional model. For narrower patches the difference is more significant. The difference between the pressure impulse down the centre line for the three-dimensional 'patch' and two-dimensional models is much larger if we move away from the centre line.

Figure 5 is a plot of pressure impulse at the base of the wall under the centre of the patch for varying values of d (the depth of the impact patch). As expected increasing the depth of impact increases the pressure impulse at the base of the wall. Figure 6 shows a plot of P/P_m offshore on the bed along the line of symmetry for a comparison of the Cooker and Peregrine two-dimensional model, and the 'patch' model with a patch of length 0.5, 1 and 2 all for $d = 0.5$ and depth of water 1. P_m is the value of P at the middle bottom of the wall. This shows that once the pressure impulse has been scaled by the value at the wall all the curves are similar in nature. However, as expected once the patch length is 1 or smaller there is a significant difference between the values predicted by the two-dimensional model and the 'patch' model.

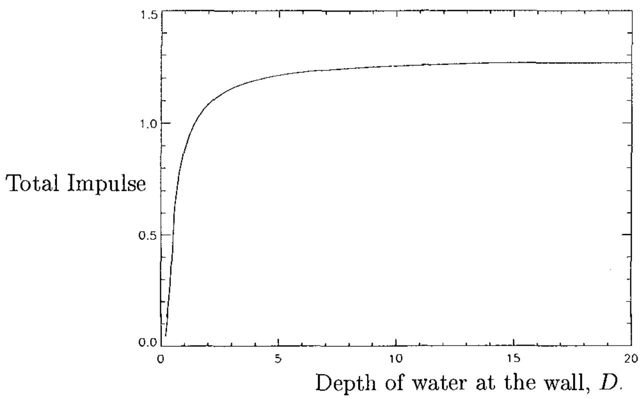

Figure 3: Total impulse against depth of water at the wall, for three-dimensional impact on a patch of a wall, where the integration is over the central width of $2a$ ($a = 1$), and the impact region is the top portion of depth 1. The total impulse has been temporarily rescaled (for this diagram only) to have the unit length scale as the depth of impact, and D as the depth of water at the wall.

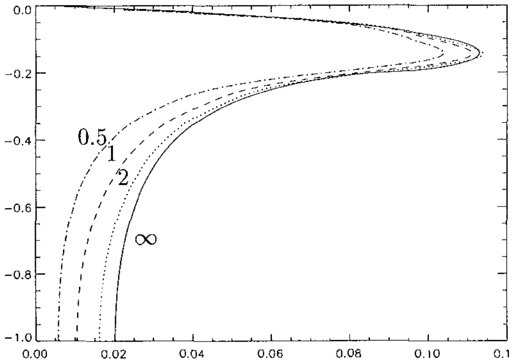

Figure 4: Pressure impulse along the centre line for the for patches of width 0.5, 1, 2, and two dimensional model (∞) of impact on a wall, with impact on the top 20%.

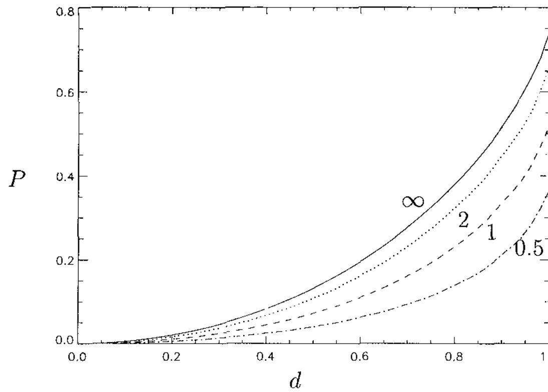

Figure 5: Pressure impulse at the base of the wall in line with the centre of the patch for patches of width 0.5, 1, 2, and two-dimensional model (∞), varying the depth of the impact region.

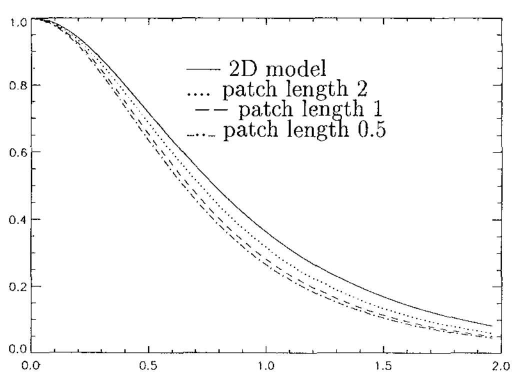

Figure 6: Plot of P/P_m offshore on the bed along the centre of the line of symmetry for a comparison of the Cooker and Peregrine two-dimensional model, and the 'patch' model with a patch of length 0.5, 1 and 2. $d = 0.5$, depth of water 1. P_m is the value of P at the middle bottom of the wall.

4. Semi-infinite patch of impact.

We need to have a clearer way of comparing the 'patch' model and the two-dimensional case. If the patch is sufficiently long, at or towards the centre of the patch the solution is the same as for the two-dimensional case. Hence, for a given length of patch, we need to estimate how far into the patch it is reasonable to assume that the solution has become two-dimensional. For a finite patch, this is difficult to assess as both ends of the patch have an effect on the solution. So we next consider a semi-infinite patch.

Figure 7 shows the problem we need to solve for impact on a semi-infinite region of the wall. We again take our length scale H as the depth of water at the wall, and work in dimensionless quantities. As we need to impose the

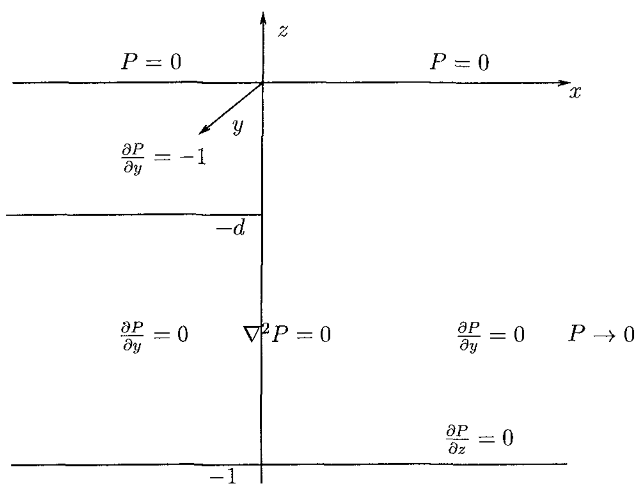

Figure 7: Impact on a semi-infinite patch of a wall. View facing wall.

forcing condition on the patch over a semi-infinite region we solve using a slightly different method to that used for the finite patch. We split the problem up into the two regions $x < 0$ and $x > 0$, the solutions to which we will denote as P_l and P_r respectively. We then use continuity of P and $\partial P/\partial x$ along the line $x = y = 0$, to find the solution. We consider first the solution in the left hand region. As $x \to -\infty$ the solution will tend to the two-dimensional solution for impact on a wall (denoted now by P_{2D}). If we subtract the solution, P_{2D}, for the two-dimensional problem off P_l then the remaining problem whose solution is P_{re} is the same as in left hand region of figure 7 except that the condition over the patch is now $\partial P/\partial y = 0$. So $P_{re} = P_l - P_{2D}$, we solve this problem for P_{re} and then $P_l = P_{re} + P_{2D}$. In a similar manner to the solution of the finite patch model we take a Fourier transform of the problem, for P_{re}, but this time the Fourier transform is a Fourier-cosine transform in the y direction (since we'll need to match with the right hand side along $x = 0$).

$$\overline{P_{re}}(x,k,z) = 2\int_0^{\infty} P_{re}(x,y,z)\cos(ky)dy. \tag{21}$$

The solution is given by:

$$P_{re} = 2\int_0^{\infty} \sum_n A_n(k)\mathrm{e}^{mx}\sin(\lambda_n z)\cos(ky)dk, \tag{22}$$

where $\lambda_n = (n+\frac{1}{2})\pi$, $m^2 = k^2 + \lambda_n^2$, and the A_n are obtained by the continuity conditions given at $x = 0$.

The solution to the two-dimensional problem (Cooker and Peregrine 1990,1992, rescaled to have the length scale as the depth of water at the wall) is given by

$$P_{2D} = -\sum_n \frac{2}{\lambda_n{}^2}\left[1-\cos(\lambda_n d)\right]\sin(\lambda_n z)\mathrm{e}^{-\lambda_n y}, \tag{23}$$

hence

$$\begin{aligned} P_l = {} & 2\int_0^{\infty} \sum_n A_n(k)\mathrm{e}^{mx}\sin(\lambda_n z)\cos(ky)dk \\ & -\sum_n \frac{2}{\lambda_n{}^2}\left[1-\cos(\lambda_n d)\right]\sin(\lambda_n z)\mathrm{e}^{-\lambda_n y}. \end{aligned} \tag{24}$$

Solution in the right hand region is similar to P_{re}. The conditions at $z = 0$, $z = -1$ and on the wall are the same. However we require P_r to be positive, and to decrease to zero as $x \to \infty$ instead of being negative and increasing to zero as $x \to -\infty$ (as P_{re}). The change in sign in front of the x is to satisfy the conditions at $x = \pm\infty$, and the negative in front of the whole expression is to ensure continuity of pressure-impulse gradient at $x = 0$. Hence P_r is given by $-P_{re}(-x,y,z)$:

$$P_r = -2\int_0^{\infty} \sum_n A_n(k)\mathrm{e}^{-mx}\sin(\lambda_n z)\cos(ky)dk, \tag{25}$$

From continuity of P at $x = 0$ we find that:

$$\begin{aligned} A_n(k) &= \frac{1}{\pi\lambda_n{}^2}\left[1-\cos(\lambda_n d)\right]\frac{\lambda_n}{k^2+\lambda_n{}^2} && k \neq 0 \\ A_n(0) &= \frac{1}{2\pi\lambda_n{}^3}\left[1-\cos(\lambda_n d)\right] && k = 0. \end{aligned} \tag{26}$$

Integration is carried out in a similar manner to that used in the evaluation of the pressure impulse for the finite patch impact. Hence P is given by equation (24) for $x < 0$ and equation (25) for $x > 0$, with A_n given in equation (26).

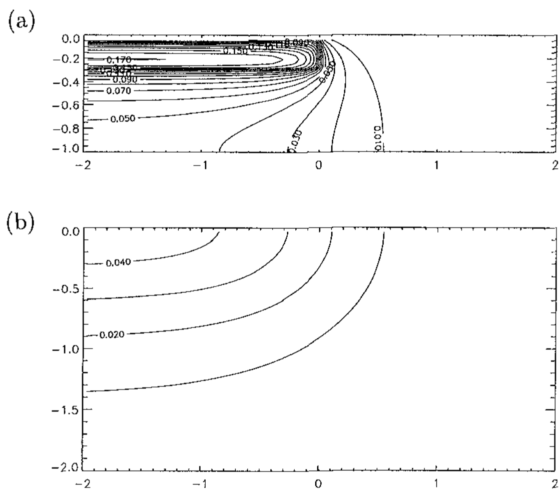

Figure 8: (a) Pressure-impulse contours, for the semi-infinite patch, on the wall for a patch of depth 0.3. (b) Pressure-impulse contours, for the semi-infinite patch, on the bed in front of the wall for a patch of depth 0.3.

Figures 8 (a) and (b) show pressure impulse contours, for the semi-infinite patch, on the wall and base respectively for a patch of depth 0.3.

When the patch is of depth 0.3 the values calculated by the two-dimensional model only approximate the three-dimensional values well at a distance into the patch of two times the depth of the water i.e. the width of influence of the boundary conditions outside of the patch is twice the depth of the water. Figure 9 is a plot of P along the bottom of the wall for different depths of patch (scaled by the two-dimensional model value). If we examine this then we can see that the depth of impact has little effect on the influence distance of the three-dimensional boundary into the patch. If we look at a distance of 0.5 into the patch (along the bottom of the wall), we can see that the pressure impulse is only approximately 0.775 and 0.850 of the two-dimensional value for patches of depth 0.2 and 1.0 respectively.

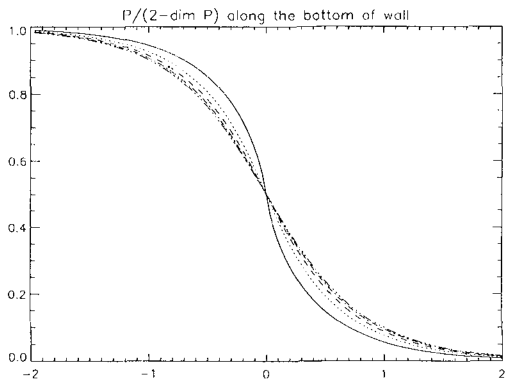

Figure 9: P/(2D value) for the semi-infinite patch as a function of position along the base of the wall, for $d = 0.2, 0.4, 0.6, 0.8, 1.0$ (from left to right in the top half of the graph).

This semi-infinite solution can be used to give an alternative derivation of the rectangular patch case, namely:

$$x > \frac{a}{2}, \quad P_r(x - \frac{a}{2}, y, z) - P_r(x + \frac{a}{2}, y, z) \tag{27}$$

$$-\frac{a}{2} < x < \frac{a}{2}, \quad P_l(x - \frac{a}{2}, y, z) - P_r(x + \frac{a}{2}, y, z) \tag{28}$$

$$x < -\frac{a}{2}, \quad P_l(x - \frac{a}{2}, y, z) - P_l(x + \frac{a}{2}, y, z) \tag{29}$$

$$\tag{30}$$

5. Conclusions

The Cooker and Peregrine (1990,1992) pressure-impulse model for impact on a plane vertical wall has been used for three-dimensional examples. The extension of this work to the impact on a semi-infinite patch of wall allowed conclusions to be drawn as to what distance into the patch we could assume two-dimensionality. The length of influence was found to be about twice that of the height of the wall. Interestingly, this distance of influence is little affected by the percentage of the water depth involved in impact. We conclude that if the wave impact width is greater than four times the height of the wall, then a two-dimensional model can be used to predict peak pressure impulse. However for waves with crest width less than twice the water depth three-dimensional effects play a significant role and should be included.

It is thought that comparison with experiment would lead to greater understanding of three-dimensional effects. However, the difficulties associated with estimating the width of the wave crest at impact from experiment means that as yet this has not been possible.

Acknowledgements

Support of the U.K. EPSRC and the European Commission, Directorate General XII, Science, Research and Development, contract number MAS3-CT95-0041, is gratefully acknowledged.

References

BAGNOLD, R.A. (1939). Interim report on wave pressure research. *J. Inst. Civil Engrs* **12**, 201-226.

BATCHELOR, G.K. (1967). *An Introduction to Fluid Dynamics* Cambridge University Press.

CHAN, E.S. (1994). Mechanics of deep water plunging-wave impacts on vertical structures. *Coastal Engng* **22**, 115-133.

COOKER, M.J. & PEREGRINE, D.H. (1990). A model for breaking wave impact pressures. *Proc. 22nd Internat. Conf. Coast. Engng., ASCE* 1473-1486.

COOKER, M.J. & PEREGRINE, D.H. (1992). Wave impact pressure and its effect upon bodies lying on the sea bed. *Coastal Engng.* **18** 205-229.

COOKER, M.J. & PEREGRINE, D.H. (1995). Pressure-impulse theory for liquid impact problems. *J. Fluid Mech.* **297** 193-214.

LAMB, H. (1932). *Hydrodynamics.* 6th Edn. Cambridge University Press.

LOSADA, M.A., MARTIN, F.L. & MEDINA, R. (1995). Wave kinematics and dynamics in front of reflective structures. *Wave forces on inclined and vertical wall structures. ASCE* editors N. Kobayashi & Z. Demirbilek 282-310

TOPLISS, M.E. (1994). Water wave impact on structures. Ph.D. dissertation, University of Bristol.

WOOD, D.J. & PEREGRINE, D.H. (1996) Wave impact beneath a horizontal surface. *Proc. 25th Internat. Conf. on Coastal Engineering Orlando, ASCE* vol 3, 2573-2583